# UC Davis
## UC Davis Previously Published Works

**Title**

Investigation of the Small Size of Nanobodies for a Sensitive Fluorescence Polarization Immunoassay for Small Molecules: 3-Phenoxybenzoic Acid, an Exposure Biomarker of Pyrethroid Insecticides as a Model

**Authors**

Wang, Yulong
Li, Zhenfeng
Barnych, Bogdan
et al.

# Investigation of Small Size of Nanobody for Sensitive Fluorescence Polarization Immunoassay for Small Molecule: 3-phenoxybenzoic Acid, an Exposure Biomarker of Pyrethroid Insecticides as a Model

**Yulong Wang**[†,‡], **Zhenfeng Li**[‡], **Bogdan Barnych**[‡], **Jingqian Huo**[‡,∥], **Debin Wan**[‡], **Natalia Vasylieva**[‡], **Junli Xu**[†], **Pan Li**[†], **Beibei Liu**[†], **Cunzheng Zhang**[*,†,§], **Bruce D. Hammock**[*,‡]

[†]Institute of Food safety and nutrition, Jiangsu Academy of Agricultural Sciences, Jiangsu Key Laboratory for Food Quality and Safety-State Key Laboratory Cultivation Base of Ministry of Science and Technology, Nanjing 210014, China

[‡]Department of Entomology and Nematology and UCD Comprehensive Cancer Center, University of California, Davis, California 95616, United States

[§]School of Food and Biological Engineering, Jiangsu University, Zhenjiang 212013, China

[∥]College of Plant Protection, Agricultural University of Hebei, Baoding 071001, China

## Abstract

Limited reports on use of nanobodies (Nbs) in fluorescence polarization immunoassay (FPIA), aroused us to explore if the small size of Nbs is a drawback for the development of sensitive FPIA to small molecular compounds, particularly since FPIA is a technology strongly dependent on molecular weight. In the present work, three different molecular weight Nbs against 3-phenoxybenzoic acid (3-PBA), an exposure biomarker of pyrethroid insecticides, including bare Nbs (15 kDa), Nbs-Avidin (Nbs-AV, 60 kDa) and Nbs-Alkaline phosphatase (Nbs-AP, 130 kDa) were specifically generated to cover distinct regions on the polarization and molecular weight relationship curve for a fluorescein tracer. In competitive FPIA, similar half-maximal inhibitory concentrations ($IC_{50}$) of 3-PBA of 16.4 ng mL$^{-1}$, 12.2 ng mL$^{-1}$ and 14.8 ng mL$^{-1}$ were obtained for Nbs, Nbs-AV and Nbs-AP, respectively, indicating that the size of Nbs in the range tested had no significant effect on the sensitivity of the resulting competitive FPIA. An $IC_{50}$ of 20.2 ng mL$^{-1}$ for an anti-3-PBA polyconal antibody based FPIA further demonstrated the performance of Nbs which was comparable to that of traditional antibodies in FPIA. Spike-recovery studies showed good and reproducible recovery of 3-PBA in urine samples, demonstrating the applicability of Nbs-based FPIA. Overall, our results show that Nbs-based FPIA achieves sensitivity levels of FPIA based on conventional antibodies and further indicate Nb absolutely meets the sensitivity requirement of FPIA.

[*]Corresponding Author. zhcz2003@hotmail.com & bdhammock@ucdavis.edu.

## Graphical Abstract
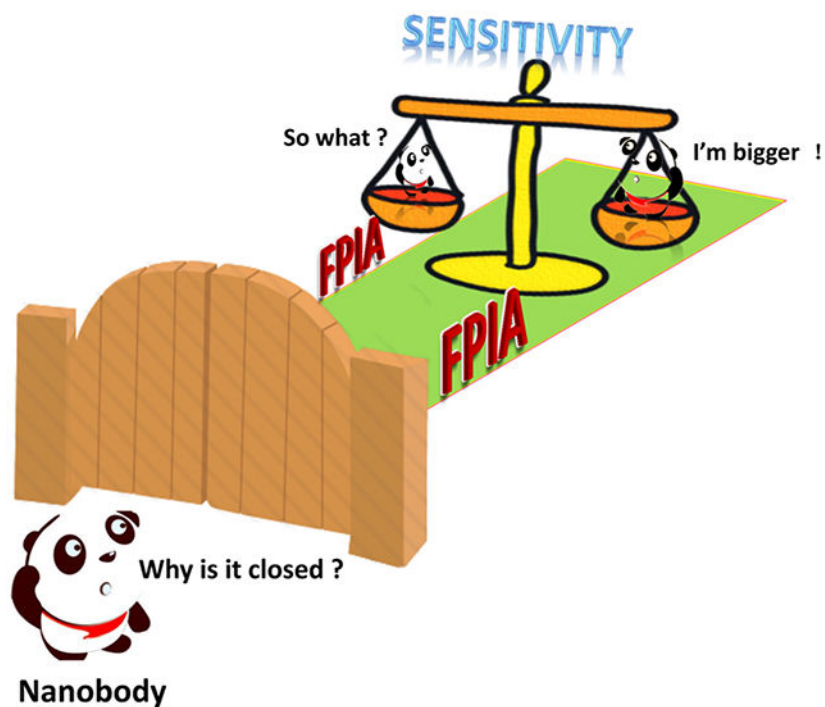


## Keywords

Fluorescence polarization immunoassay; Nanobody; Insecticide; 3-phenoxybenzoic acid; Fluorescein

## 1. INTRODUCTION

Nanobodies (Nbs), also referred to as single domain antibodies (VHH), are a recombinant form of heavy-chain-only antibodies, have emerged as a versatile alternative for conventional IgGs since they were first reported in 1993.[1] Although Nbs possess only a single variable domain, their affinity and specificity for target molecule compares favorably with traditional IgGs.[2] Their small size, high conformational stability, and ease of recombinant modification and production not only trigger the current bloom of therapeutic applications of Nbs but also create and boost novel immunoassays.[3]

The small size ($\approx$ 15 kDa; $\approx$ 4 nm $\times$ 2.5 nm $\times$ 3 nm), a canonical representation of Nbs, endows advantages in different immuno-based applications, such as *in vivo* molecular imaging,[4,5] biosensor development and homogeneous Förster resonance energy transfer (FRET)-based immunoassays.[6,7] In tumor imaging, the small size of Nbs is advantageous in terms of tumor penetration, rapid biodistribution and tumor labeling, which results in short time imaging and high-contrast images.[5,8] In addition, the reduced size contributes to higher antibody-coating density on the sensor surface, which was shown to improve the biosensor performance.[6] In FRET-based immunoassays, the small Nb size has been shown to reduce the distance between two fluorophores, thus resulting in higher FRET effciency.[7] The tiny

size renders Nbs, not just alternatives to traditional antibodies, but in some cases, the outstanding property of Nbs allows higher performances that cannot be accomplished with traditional antibodies.

Recently, Nbs have been used in a plethora of assay formats,[6,7,9,10] yet the use of Nbs in fluorescence polarization immunoassays (FPIA) is rare. Thus, an obvious question arises: is there any limitation of Nb use in FPIA? Since the FPIA is a molecular mass sensitive analytical technique, without doubt is, the molecular size of Nbs is the first and most probable suspect. This inspired us to investigate whether the small size of Nbs is a hindrance in achieving high-performance FPIA, i.e., high sensitivity.

FPIA, a homogeneous assay technique, is mainly used for the rapid monitoring of low molecular weight compounds, including drugs in clinical diagnostics, pollutants and toxins in environmental and food control.[11–14] FPIA offers significant advantages in terms of being separation free with easy of automation, resulting in high-throughput and fast processing. The steady-state fluorescence polarization signal ($P$) depends on the excited state lifetime $\tau$ and the Debye rotational relaxation time $\rho$ of a fluorescently labeled molecule, and can be expressed by the well-known Perrin equation: $\frac{1}{P} - \frac{1}{3} = \left(\frac{1}{P_0} - \frac{1}{3}\right)\left(1 + \frac{3\tau}{\rho}\right)$, where $P_0$ is the intrinsic polarization.[13,15] For a spherical molecule, the Debye rotational relaxation time $\rho$ can be formulated as: $\rho = \frac{3\eta V}{RT}$, where $\eta$ is the viscosity, $V$ is the molar volume of the rotating molecule, $R$ is the gas constant, $T$ is the absolute temperature.[11,14] In a constant solution system (constant $\eta$, $R$ and $T$) with a fixed fluorophore (constant $\tau$), the $P$ is proportional to the molecular volume or the molecular mass. That is to say the polarization of a rotating fluorophore is low when it is attached to a small species, but is high with a large one. In a competitive FPIA, the analyte competes with a small fluorescent-labeled antigen (tracer) for the limited binding site of a specific antibody, resulting in a decrease in the degree of light polarization value.[16,17]

To get high sensitivities, a significant difference between the polarization value of the bound and free tracers is required. However, a molecule with molecular weight of 15 kDa appears not to get a saturated polarization value according to previous studies.[18] Thus when a Nb is used in FPIA, the contribution of the polarization difference to the sensitivity is not clear, since the sensitivity of a competitive immunoassay system is intricately determined by the concentration of competitive antigen and/or antibody, the heterogeneity of antigen, the affinity of antibody and the properties of signal tags, etc.[19,20] An anchor protein module concept was used to increase the size of aptamer receptors in fluorescence polarization aptamer assay for ochratoxin A with an enhancement of assay sensitivity.[21]

On these basis, three different molecular weight Nbs were developed to make a sensitivity comparison of their corresponding competitive FPIAs. The molecular weight of three selected Nbs were specifically chosen at three representative points of polarization-molecular weight relationship curve for fluorescein tracer,[18] which were at fast-rising point of that curve (15 kDa), approach to saturation point (60 kDa) and saturation point (130 kDa), respectively. The three Nbs against 3-phenoxybenzoic acid (3-PBA) were generated by recombinant fusion technology, including bare Nbs (15 kDa), Nbs-Avidin (Nbs-AV, 60 kDa)

and Nbs-Alkaline phosphatase (Nbs-AP, 130 kDa). The use of recombinant fusion protein alleviates the need to prepare chemical conjugates via chemical labeling with different substances (e.g. proteins or metal nanoparticles), which sometimes damages the activity of antibody and may result in highly heterogeneous conjugates due to difficulty in controlling binding ratio. The performance of the Nbs in competitive FPIA by quantitative detection of 3-PBA, which is considered as a metabolic biomarker of many pyrethroid insecticides[22] (Figure 1A), was evaluated in detail. Finally, a Nbs-based FPIA was used to analyze 3-PBA in the urine.

## 2. MATERIALS AND METHODS

### 2.1. Chemicals

DNA polymerase, nicking enzyme, T4 DNA ligase and $10 \times$ CutSmart buffer were obtained from New England Biolabs (Beverly, MA, USA). Bacterial-protein-extraction reagent (B-PER), NuPAGE Bis-Tris gel and HisPur Ni-NTA resin were purchased from Thermo Fisher Scientific (Rockford, IL, USA). The pET 22b (+) vector containing the Rhizavidin (RZavidin) fragment and pecan45 vector containing the alkaline phosphatase (AP) fragment were generously provided by Dr. Ellen R. Goldman (Naval Research Laboratory, DC, USA). 3-Phenoxybenzoic acid (3-PBA) was purchased from Sigma Aldrich (St. Louis, MO, USA). The hapten 3-(4-methoxyphenoxy)-benzoic acid was previously synthesized in our laboratory at UC Davis (University of California Davis, CA, USA). AMF [4'-(Aminomethyl)fluorescein] was obtained from AAT Bioquest, Inc. (Sunnyvale, CA, USA). Polyclonal antibodies and nanobody genes were previously obtained in our lab.[22,23]

### 2.2. Generation of Nbs

Recombinant plasmids encoding the bare Nbs, Nbs–AV and Nbs–AP fusion proteins with 6 × His tags at the C-terminus were constructed, respectively, using classical gene recombination technology including gene amplification, enzyme digestion and ligation (details in Supporting Information). Few single colonies of the transformed cells were picked and sequenced at the UC Davis DNA Sequencing Facility. The target plasmid was transformed into *Escherichia coli* BL21 (DE3) plysS cells to induce the protein expression in an auto-induction media. The cells containing target fusion protein were lysed by using the bacterial protein extraction reagent kit (B-PER) followed by purification on a 1 mL Ni-NTA resin column. The size and purity of those Nbs were determined by sodium dodecyl sulfate-polyacrylamide gel electrophoresis (SDS-PAGE) (Figure 2).

### 2.3. Synthesis of Tracer Antigen

The tracer antigen conjugate was synthesized by the Schiff base formation of the amino group of fluorescein with the aldehyde group of the hapten (Figure 1B). Briefly, 11 mg of 3-PBA hapten was dissolved in 1 mL of N,N-dimethylformamide and mixed with 4 mg 4′-(Aminomethyl)fluorescein (4-AMF) with gentle stirring for 1 h at room temperature (RT) in dark place. Then 10 μL of 5 M cyanoborohydride in 1 N NaOH was added to the mixture for an additional 4 h stirring in dark at RT.

The resulting yellow solution was purified by thin-layer chromatography (TLC) with a mobile phase of $CH_2Cl_2$: $CH_3OH$ (3:2, $v/v$). The band with a retention factor ($R_f$) of 0.55 was collected and dissolved in methanol. The tracer antigen conjugate was characterized by mass spectrometry and fluorescence polarization value test using a specific anti-3-PBA polyclonal antibody, respectively.

### 2.4.  FPIA Protocols

The competitive FPIA was carried out with 3-PBA standard solutions or spiked samples in the presence of tracer antigen conjugate and the anti-3-PBA Nbs at the optimized concentrations. Briefly, 70 μL of the tracer antigen conjugate, 70 μL of antibody solution and 70 μL of sample solution were mixed and incubated in a 96-well black polystyrene microplate for 15 min. A blank control was also measured using borate buffer (BB, 0.05 M, pH 8.0). The fluorescence polarization (FP) value was measured in the fluorescence polarization mode at $\lambda_{ex} = 485$ nm and $\lambda_{em} = 530$ nm by a TECAN Infinite M1000 Pro multimode microplate reader (Hombrechtikon, Switzerland).

The standard inhibition curve with the x-axis being 3-PBA concentration and the y-axis the normalized FP value ($mP/mP_0$, where mP is the FP value in the presence of 3-PBA and $mP_0$ is the FP value of the control), was plotted in Origin 8.5 software (OriginLab, MA, USA) with a four-parameter logistic equation for line fitting:

$$Y = A_2 + (A_1 + A_2)/[1 + (X/X_0)^P]$$

where Y represents the binding rate ($mP/mP_0$), X is the concentration of 3-PBA, $A_1$ and $A_2$ are the binding rates at saturated analyte concentration and zero analyte concentration, $X_0$ is the concentration of 3-PBA at 50% of binding rate ($EC_{50}$) and P is the slope at $EC_{50}$ point.

### 2.5.  Analysis of Urine Samples

Urine samples collected from healthy volunteers of our laboratory were used to test the recovery. Urine samples of 3-PBA free certified by LC-MS were spiked with 3-PBA at concentration of 100 and 400 ng mL$^{-1}$, respectively. After 20-fold dilution with BB, the solutions were analyzed by Nbs-based FPIA. For method comparison purposes, 50 μL of these samples were mixed with 50 μL of 200 nM 12-(3-cyclohexyl-ureido)-dodecanoic acid in methanol prior to LC-MS analysis for 3-PBA. Quantification was performed using Masslynx 4.1 software with TargetLynx.

For real sample analysis, urine samples collected from healthy population with no known exposure to pyrethroids, and from farm workers actively using pesticides in daily practice (provided by Dr. S. Hongsibsong from Chiang Mai University) were completely hydrolyzed with concentrated hydrochloric acid according to a previous study.[24] The hydrolyzed products by appropriate pH value adjustment (pH at 8.0 for FPIA and 6.0 for LC-MS) were used in Nbs-based FPIA and LC-MS.

## 3. RESULTS AND DISCUSSION

### 3.1. Characterization of Tracer Antigen Conjugate

The design of tracer antigen conjugate is a critical step in FPIA development. A fluorescein analogue 4′-(Aminomethyl)fluorescein (4-AMF) with a fluorescence lifetime of 4 ns was specifically selected as the fluorescence reporter due to relatively sharp fluorescence polarization-molecular weight correlation curve and availability of this group of dyes.[18] A hapten for 3-PBA with a handle attached to the 4-position of distal phenyl group has been shown to give highly sensitive immunoassays according to our previous reports.[22] The 3-PBA hapten conjugated to 4-AMF fluorescein to form Schiff base complex was firstly characterized and purified by TLC, which had a distinctive yellow band with retention factor ($R_f$) of 0.55 (Figure S1A). The MS/MS spectra results showed an expected peak at $m/z$ ([M + 1]+) 618.3 (data not shown). From the fluorescence polarization (FP) test, the tracer conjugate showed obvious binding to the specific polyclonal antibody against 3-PBA (Figure S1B), indicating the successful synthesis of the tracer conjugate.

### 3.2. Identification of Nbs

Polarization-molecular weight relationship curve for fluorescein tracer shows a sharp increase of polarization value as the molecular weight increases from 0 to nearly 30 kDa, nearly saturation at the molecular weight range of 30 ~ 100 kDa and complete saturation above 100 kDa (Figure 3a).[18] Thus, to investigate the effect of antibody size on the sensitivity of FPIA, we picked one point in each range as follows: 15 kDa, 60 kDa and 130 kDa, respectively. Rhizavidin and alkaline phosphatase were selected as fusion partners for recombinant expression of Nbs-Avidin (Nbs-AV, 60 kDa) and Nbs-Alkaline phosphatase (Nbs-AP, 130 kDa) dimer fusion proteins based on genetic fusion protein technology. Both the rhizavidin and alkaline phosphatase have proven to be good fusion partners for recombinant antibody production with good yield and stability.[25,26] In addition, Nbs have been widely utilized in recombinant antibodies, as an alternative to traditional single chain antibody (scFv) due to their excellent solubility and ability to refold after denaturation.[27,28]

Genetic fusions allow one to finely tune molecular weight of the resulting fusion protein, while retaining the recognition ability against analyte. Meanwhile, genetic fusions remove the need to prepare chemical conjugates which sometimes show disadvantages in terms of high heterogeneity and reduced antibody activity.[25] The constructed recombinant plasmids of Nb were confirmed by PCR and DNA sequencing, respectively. Positive recombinant plasmids were transformed into *E. coli* BL21 (DE3) cells for protein expression and the resulting Nbs were purified using a Ni-NTA affinity column. The size and purity of the proteins were verified on NuPAGE 12% Bis-Tris Protein gel (Thermo Fisher, USA), where the purified Nbs, Nbs–AV and Nbs–AP fusion proteins showed the expected bands of approximately 15 kDa, 30 kDa and 65 kDa, respectively (Figure 2). The binding characteristics of the original Nb were preserved in the fusion proteins as shown in the competitive ELISA experiments (data not shown).

### 3.3. Analytical Characterization

Under the optimized conditions (optimized concentration of tracer and antibodies, Supporting Information), the half-maximal inhibitory concentration ($IC_{50}$) levels obtained by the competitive FPIA based on sigmoidal inhibition curves were 16.4 ng mL$^{-1}$, 12.2 ng mL$^{-1}$ and 14.8 ng mL$^{-1}$ for Nbs, Nbs–AV and Nbs-AP, respectively (Figure 4). It appears that similar $IC_{50}$s are indicative of negligible effect of Nb size on the sensitivity (at MW > 15 kDa) (here "sensitivity" is straightforward expressed as $IC_{50}$) of a competitive FPIA.

In a typical competitive immunoassay system, the sensitivity has been empirically proven to be associated with the concentration and affinity/avidity of antibody and antigen (even subdivided to associate with the valence and the heterogeneity of antibody and/or competitive antigen) as well as properties of signal tags.[19,20,29,30] In our FPIA system, we used one kind monovalent tracer (1:1 molar ratio of 3-PBA hapten and 4-AMF fluorescein), thus eliminating the variability associated with the change of antigen structure, the valence of antigen and quantum yield of signal tags. The Nbs and two Nbs fusion proteins had very similar affinity constants ($K_d$ = 17 nM for bare Nbs, $K_d$ = 12 nM for Nbs-AV and $K_d$ = 15 nM for Nbs-AP, Supporting Information), which is not surprising based on the fact that all three proteins have the same protein sequence of the binding domain. The affinity of Nbs-AV and Nbs-AP was slightly higher than that of bare Nbs was probably due to the dimer nature of those fusions (avidity contribution). The increased affinity of the two fusion Nbs is attributed to the increase in sensitivity resulted from the formation of divalent complex. This further indicates the negligible effect of Nbs size (at MW > 15 kDa) on sensitivity of the competitive FPIA.

In addition, the sensitivity ($IC_{50}$) of traditional polyclonal antibody (Pab) based FPIA was 20.2 ng mL$^{-1}$ (Figure 4) and compared well with the Nbs-based FPIA. This result was consistent with the trend result we previously reported for corresponding ELISAs (ELISA $IC_{50}$ (Pab) = 1.65 ng mL$^{-1}$; $IC_{50}$ (Nb) = 1.4 ng mL$^{-1}$).[21,22] The empirical observation that FPIAs have one order of magnitude lower sensitivity compared to classical ELISAs[16,31] seem to hold for the assay developed here as well.

In summary, the Nb size has no significant effect on the sensitivity of a competitive FPIA at least for fluorescein-based reporters, but probably more generally for reporters with lifetimes 4 ns. Additionally, Nbs-based FPIA shows comparable sensitivity to traditional Pab-based FPIA. All this indicates that Nbs absolutely meet the sensitivity requirement of FPIA that traditional antibody achieves and are expected to boost the development of Nbs-based FPIA.

### 3.4. Nbs-based FPIA on Urine Samples

3-PBA is a common urinary metabolite of pyrethroids in mammals, which was shown to be a biomarker of human exposure to pyrethroids.[22] In the present study, urine was selected to evaluate the performance of the Nbs-based FPIA as well as the recovery of 3-PBA from spiked urine samples. Different concentrations of 3-PBA at 100 ng mL$^{-1}$ and 400 ng mL$^{-1}$ were spiked into urine from healthy volunteers, respectively. To reduce the matrix effect of urine samples, the spiked sample solutions were diluted 20-fold prior to for FPIA (Figure S3). Table 1 shows the average recovery values (n = 5) of 89% with coefficients of variation

(CV) below 6.7%. The recovery results of the spiked samples obtained by Nbs-based FPIA are in good agreement with those obtained by LC-MS, confirming the reliability and practicability of this Nbs-FPIA for 3-PBA analysis. As shown in Table S1, positive real urine samples containing concentrations of 3-PBA higher than 50.6 ng mL$^{-1}$ are accurately detected by the developed Nbs-FPIA. To detect lower concentrations of 3-PBA, sample preparation by solid-phase extraction (SPE) or a mixed-mode SPE method should be recommended to be used.[23]

In this study, we investigated the effect of nanobody (Nb) size on the sensitivity of fluorescence polarization immunoassay (FPIA). Three different molecular weight Nbs against 3-phenoxybenzoic acid (3-PBA) were specifically generated to cover distinct regions on the polarization-molecular weight relationship curve for fluorescein tracer. Similar half-maximal inhibitory concentration (IC$_{50}$) levels of the three different molecular weight Nbs indicated that the size of Nbs had no significant effect on the sensitivity of the competitive FPIA. Comparable sensitivities between Pab- and Nb-based FPIAs further pointed at the value of Nb as an alternative for the development of FPIA. Application of Nbs-based FPIA to the analysis of spiked urine and real urine samples showed excellent recoveries of 3-PBA analyte and good correlation with LC-MS results. It appears that the scarcity of reports on the application of Nbs in FPIA is not related to their relatively small molecular weight (and thus poor sensitivity), but rather to other reasons like limited availability of Nbs particularly to small molecular compounds which proved to be hard targets due to the high failure rate of Nb generation and failure to compete the small molecule reporter off of the Nb. We hope that our research will boost the development of Nbs-based FPIAs, but also lead to significant improvements in this field by taking advantage of outstanding properties of Nbs, which make them stand out as unique analytical tools.

## Supplementary Material

Refer to Web version on PubMed Central for supplementary material.

## Acknowledgments

## REFERENCES

(1). Hamers-Casterman C; Atarhouch T; Muyldermans S; Robinson G; Hamers C; Songa EB; Bendahman N; Hammers R Naturally occurring antibodies devoid of light chains. Nature 1993, 363, 446–448. [PubMed: 8502296]

(2). Bever CS; Dong JX; Vasylieva N; Barnych B; Cui YL; Xu ZL; Hammock BD; Gee SJ VHH antibodies: emerging reagents for the analysis of environmental chemicals. Anal. Bioanal. Chem 2016, 408, 5985–6002. [PubMed: 27209591]

(3). Gonzalez-Sapienza G; Rossotti MA; Tabares-da Rosa S Single-domain antibodies as versatile affinity reagents for analytical and diagnostic applications. Front. Immunol 2017, 8, 977. [PubMed: 28871254]

(4). Chakravarty R; Goel S; Cai W Nanobody: the "magic bullet" for molecular imaging? Teranostics 2014, 4, 386–398.

(5). Hoefman S; Ottevaere I; Baumeister J; Sargentini-Maier M Pre-clinical intravenous serum pharmacokinetics of albumin binding and non-half-life extended nanobodies. Antibodies 2015, 4, 141.

(6). Zhou Y; Hu W; Peng B; Liu Y Biomarker binding on an antibody-functionalized biosensor surface: the influence of surface properties, electric field, and coating density. J. Phys. Chem. C 2014, 118, 14586–14594.

(7). Wegner KD; Lindén S; Jin Z,W; Jennings T,L; El Khoulati R; Van Bergen En Henegouwen P,M,P; Hildebrandt N. Nanobodies and nanocrystals: highly sensitive quantum dot-based homogeneous FRET immunoassay for serum-based EGFR detection. Small 2014, 10, 734–740. [PubMed: 24115738]

(8). Revets H; De Baetselier P; Muyldermans S Nanobodies as novel agents for cancer therapy. Expert Opin. Biol. Ter 2005, 5, 111–124.

(9). Goode J; Dillon G; Millner PA The development and optimisation of nanobody based electrochemical immunosensors for IgG. Sensor. Actuat. B-Chem 2016, 234, 478–484.

(10). Doerflinger SY; Tabatabai J; Schnitzler P; Farah C Development of a nanobody-based lateral flow immunoassay for detection of human norovirus. mSphere 2016, 1, 1–6.

(11). Jameson DM; Ross JA Fluorescence polarization/anisotropy in diagnostics and imaging. Chem. Rev 2010, 110, 2685–2708. [PubMed: 20232898]

(12). Boroduleva AY; Wu J; Yang QQ; Li H; Zhang Q; Li PW; Eremin SA Development of fluorescence polarization immunoassays for parallel detection of pesticides carbaryl and triazophos in wheat grains. Anal. Methods 2017, 9, 6814–6822.

(13). Perrier S; Guieu V; Chovelon B; Ravelet C; Peyrin E Panoply of Fluorescence Polarization/ Anisotropy Signaling Mechanisms for Functional Nucleic Acid-Based Sensing Platforms. Anal. Chem 2018, 90, 4236–4248. [PubMed: 29513518]

(14). Burke TJ; Loniello KR; Beebe JA; Ervin KM Development and application of fluorescence polarization assays in drug discovery. Comb. Chem. High T Scr 2003, 6, 183–194

(15). Perrin F Vie moyenne des molécules dans l'etat excité. J. Phys. (Paris) 1926, 7, 390.

(16). Dong BL; Zhao SJ; Li HF; Wen K; Ke YB; Shen JZ; Zhang SY; Shi WM; Wang ZH Design, synthesis and characterization of tracers and development of a fluorescence polarization immunoassay for the rapid detection of ractopamine in pork. Food Chemistry 2019, 271, 9–17. [PubMed: 30236746]

(17). Pennacchio A; Varriale A; Scala A; Marzullo VM; Staiano M; D'Auria S A novel fluorescence polarization assay for determination of penicillin G in milk. Food Chemistry 2016, 190, 381–385. [PubMed: 26212986]

(18). Owicki JC Fluorescence polarization and anisotropy in high throughput screening: perspectives and primer. J. Biomol. Screen 2000, 5, 297–306. [PubMed: 11080688]

(19). Goodrow MH; Hammock BD Hapten design for compound-selective antibodies: ELISAS for environmentally deleterious small molecules. Anal. Chim. Acta 1998, 376, 83–91.

(20). Vasylieva N; Barnych B; Rand A; Inceoglu B; Gee SJ; Hammock BD Sensitive immunoassay for detection and quantification of the neurotoxin, tetramethylenedisulfotetramine. Anal. Chem 2017, 89, 5612–5619. [PubMed: 28398746]

(21). Samokhvalov AV; Safenkova IV; Eremin SA; Zherdev AV; Dzantiev BB Use of anchor protein modules in fluorescence polarisation aptamer assay for ochratoxin A determination. Anal. Chim. Acta 2017, 962, 80–87. [PubMed: 28231883]

(22). Shan GM; Huang HZ; Stoutamire DW; Gee SJ; Leng G; Hammock BD A sensitive class specific immunoassay for the detection of pyrethroid metabolites in human urine. Chem. Res. Toxicol 2004, 17, 218–225. [PubMed: 14967009]

(23). Kim HJ; McCoy MR; Majkova Z; Dechant JE; Gee SJ; Tabares-da Rosa S; González-Sapienza GG; Hammock BD Isolation of alpaca anti-hapten heavy chain single domain antibodies for development of sensitive immunoassay. Anal. Chem 2012, 84, 1165–1171. [PubMed: 22148739]

(24). Leng G; Leng A; Kuhn KH; Lewalter J; Pauluhn J Human dose-excretion studies with the pyrethroid insecticide cyfluthrin: urinary metabolite profile following inhalation. Xenobiotica 1997, 27, 1273–1283. [PubMed: 9460232]

(25). Liu JL; Zabetakis D; Walper SA; Goldman ER; Anderson GP Bioconjugates of rhizavidin with single domain antibodies as bifunctional immunoreagents. J. Immunol. Methods 2014, 411, 37–42. [PubMed: 24946086]

(26). Liu X; Xu Y; Wan DB; Xiong YH; He ZY; Wang XX; Gee SJ; Ryu D; Hammock BD. Development of a nanobody-alkaline phosphatase fusion protein and its application in a highly sensitive direct competitive fluorescence enzyme immunoassay for detection of ochratoxin A in cereal. Anal. Chem 2015, 87, 1387–1394. [PubMed: 25531426]

(27). Eyer L; Hruska K Single-domain antibody fragments derived from heavy-chain antibodies: a review. Vet. Med 2012, 57, 439–513.

(28). Holliger P; Hudson PJ Engineered antibody fragments and the rise of single domains. Nat. Biotechnol 2005, 23, 1126–1136. [PubMed: 16151406]

(29). Oda M; Sato-Nakamurab N; Azuma T. Molecular characterization of monovalent and multivalent hapten–protein conjugates for analysis of the antigen–antibody interaction. Anal. Biochem 2004, 333, 365–371. [PubMed: 15450814]

(30). Oda M; Uchiyama S; Noda M; Nishi Y; Koga M; Mayanagi K; Robinson CV; Fukui K; Kobayashi Y; Morikawa K; Azuma T. Effects of antibody affinity and antigen valence on molecular forms of immune complexes. Mol. Immunol 2009, 47, 357–367. [PubMed: 19800690]

(31). Li C; Zhang YY; Eremin SA; Yakup O; Yao G; Zhang XY Detection of kanamycin and gentamicin residues in animal-derived food using IgY antibody based ic-ELISA and FPIA. Food Chemistry 2017, 227, 48–54. [PubMed: 28274457]
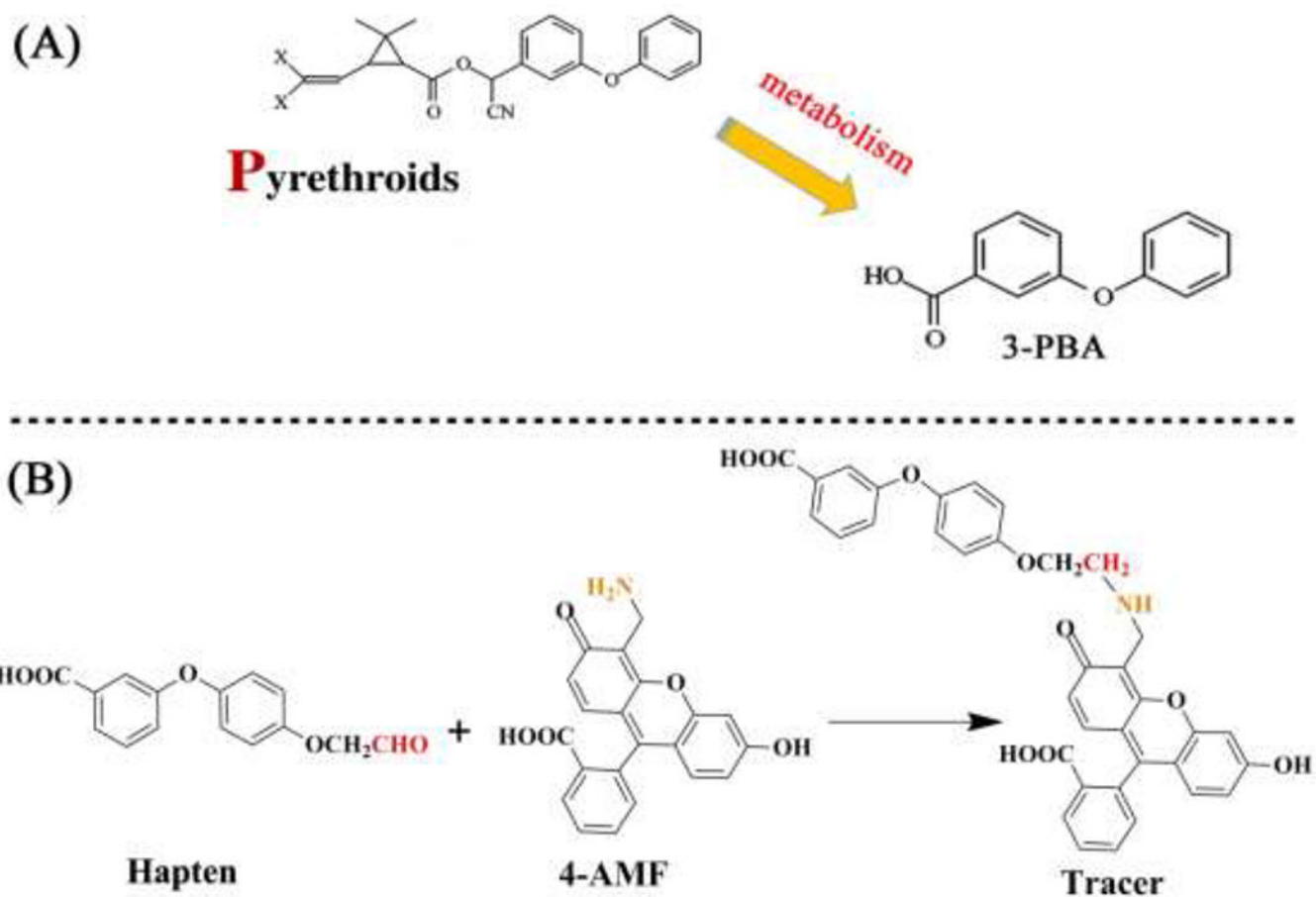
**Figure 1.**
(A) Structures of pyrethroid and its metabolite 3-PBA and (B) Synthetic scheme of tracer antigen conjugate synthesis using a 3-PBA hapten and 4′-(Aminomethyl)fluorescein (4-AMF).
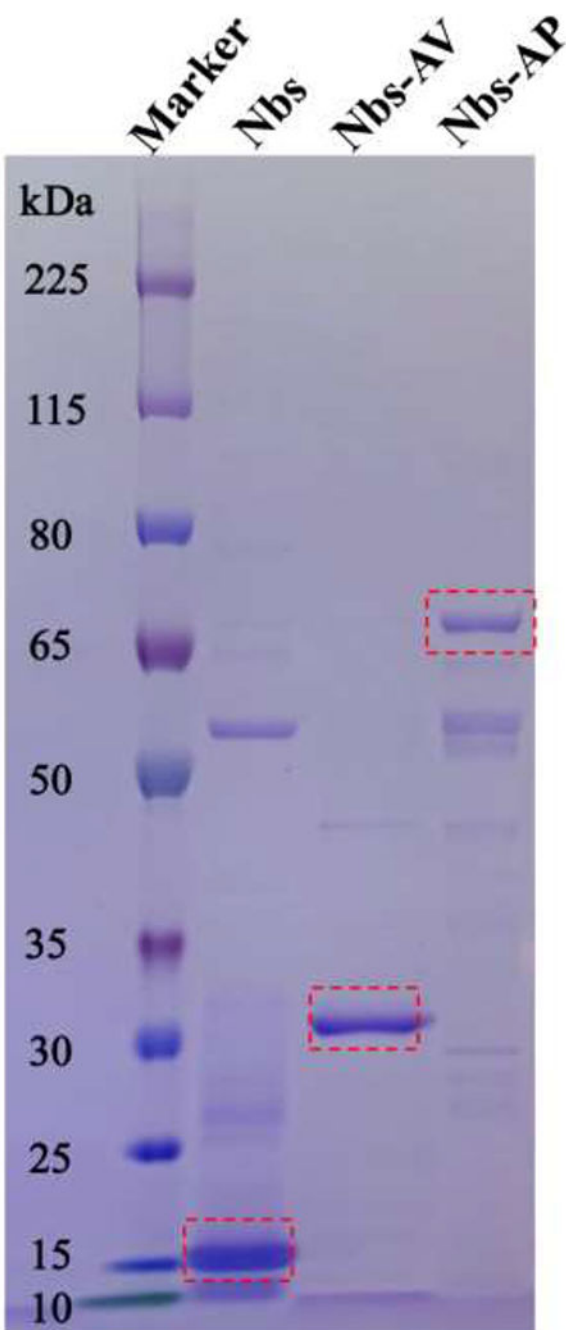
**Figure 2.**
SDS-PAGE analysis of the Nbs, Nbs-AV and Nbs-AP proteins. Red dashed squares show the target band of each antibody. Blots were stained with SYPRO Ruby protein-gel stain.
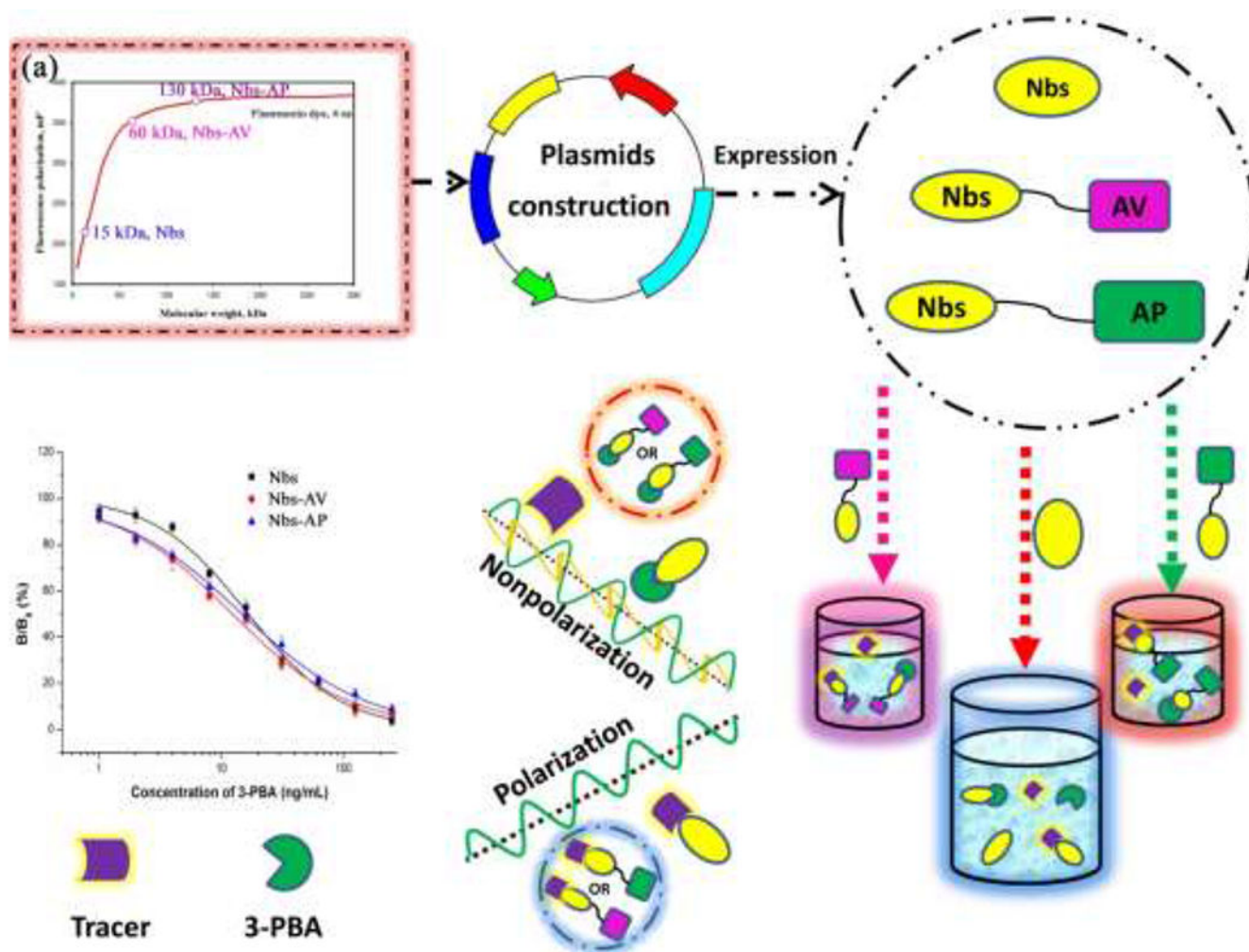
**Figure 3.**
Schematic illustration of the different sized Nbs for 3-PBA FPIA. In a homogeneous FPIA, the analyte 3-PBA and fluorescent tracer antigen conjugates competed for the binding sites of the anti-3-PBA Nbs. As a result of competition, the polarization signal was inversely proportion to the concentration of 3-PBA. Specific sized Nbs construction were guided by the relationship curve between polarization and molecular weight for fluorescein tracer to cover distinct regions of the curve (insert figure (a) was adapted with permission from Ref. 18 (Copyright [SAGE Publications], [2000]).
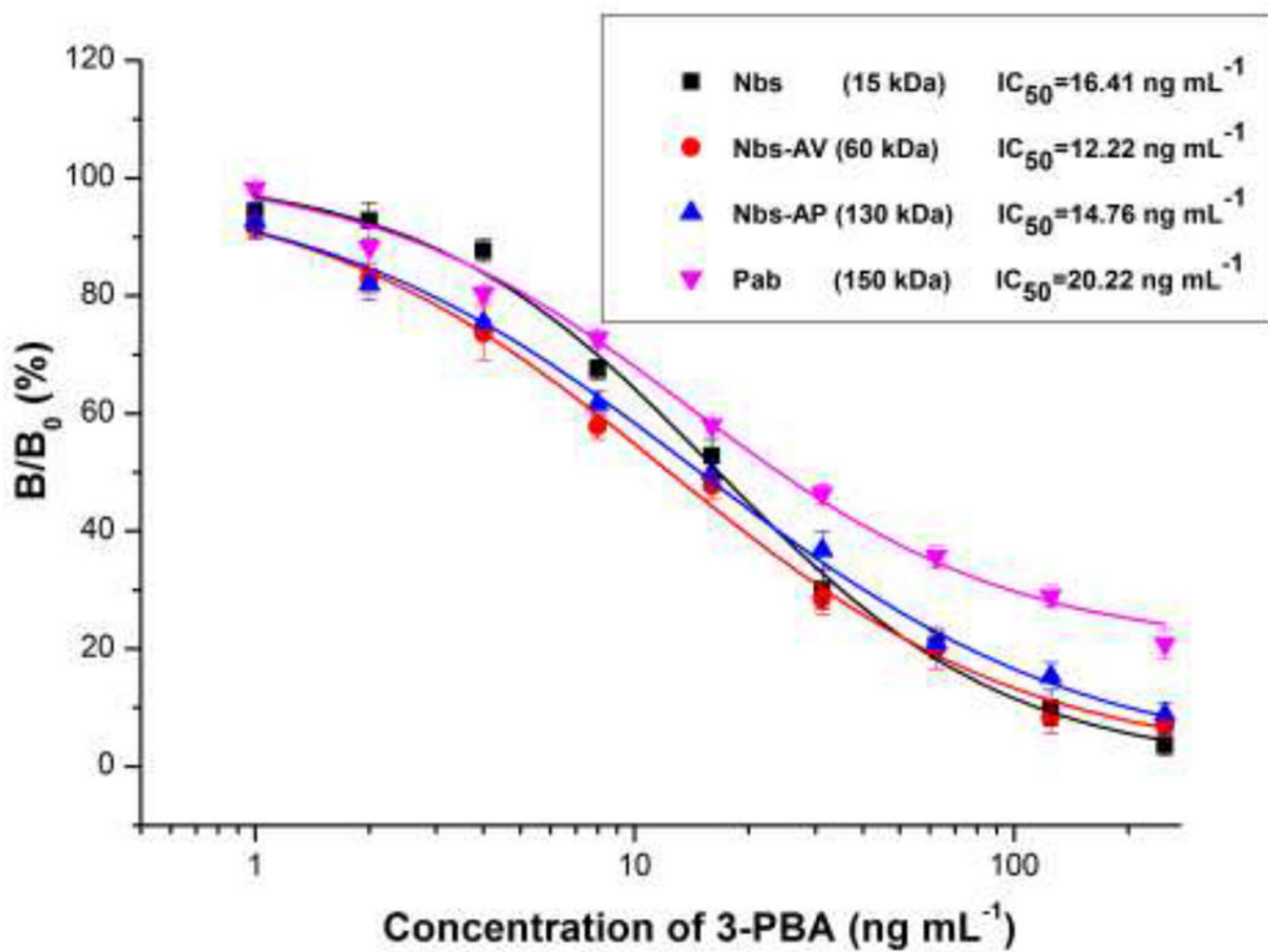
**Figure 4.**
Standard inhibition curve for different size antibodies (Nbs, Nbs-AV, Nbs-AP and Pab) in FPIA for 3-PBA.

**Table 1.**

Comparison of Performance of Nbs-FPIA and LC-MS for Quantification of 3-PBA in Urine (n = 5)

| Spiked concentration (ng mL$^{-1}$) | Nbs-FPIA | | | LC-MS | | |
|---|---|---|---|---|---|---|
| | Found±SD$^a$ (ng mL$^{-1}$) | Recovery (%) | CV$^b$ (%) | Found±SD (ng mL$^{-1}$) | Recovery (%) | CV (%) |
| 100 | 89±6 | 89 | 6.7 | 84±8 | 84 | 9.5 |
| 400 | 356±15 | 89 | 4.2 | 368±7 | 92 | 1.9 |

[a] Mean measured concentration of five replicates ± standard deviation.

[b] Coefficient of Variation of five measurements.